

## Langevin dynamics of polymeric manifolds in melts

This article has been downloaded from IOPscience. Please scroll down to see the full text article.

1999 J. Phys.: Condens. Matter 11 A307

(<http://iopscience.iop.org/0953-8984/11/10A/028>)

View [the table of contents for this issue](#), or go to the [journal homepage](#) for more

Download details:

IP Address: 129.252.86.83

The article was downloaded on 27/05/2010 at 11:26

Please note that [terms and conditions apply](#).

# Langevin dynamics of polymeric manifolds in melts

V G Rostiashvili<sup>†‡</sup>, M Rehkopf<sup>†</sup> and T A Vilgis<sup>†</sup>

<sup>†</sup> Max-Planck-Institut für Polymerforschung, Postfach 3148, D-55021 Mainz, Germany

<sup>‡</sup> Institute of Chemical Physics, Russian Academy of Science, 142432, Chernogolovka, Moscow Region, Russia

Received 2 October 1998

**Abstract.** The Martin–Siggia–Rose generating functional (MSR-GF) technique is used for treating the polymeric  $D$ -dimensional-manifold melt dynamics. The one- (test-) manifold dynamics and the collective dynamics are considered separately. The test-manifold dynamics is obtained by integrating out the melt collective variables. This is done within the dynamic random-phase approximation (RPA). The resulting effective-action functional of the test manifold is treated by making use of the self-consistent Hartree approximation. As a consequence, the generalized Rouse equation of the test manifold is derived, and its static and dynamic properties are studied. By making use the MSR-GF technique, the fluctuations around the RPA of the collective variables—mass density and response-field density—are investigated. As a result, the equations for the correlation and response functions are derived. The memory kernel can be specified for the ideal glass transition as a sum of all ‘water-melon’ diagrams.

## 1. Introduction

When we extend a treatment of an isolated polymer chain (or more generally a  $D$ -dimensional polymeric manifold) to a polymeric melt of identical species, two general theoretical problems arise.

The first is related to the one- (test-) chain dynamics: how are the coefficients of the Rouse equation (for chains shorter than the entanglement length  $N_e$ ) renormalized? This question does not at first sight seem apposite, since it is known from experiments [1] that the Rouse model itself provides a good description for the melt of the relatively short chains with  $N < N_e$ . On the other hand, novel investigations by means of molecular dynamics (MD) simulations and neutron spin-echo spectroscopy have shown systematic deviations from the Rouse behaviour [2, 3] and suggest such a renormalization. This actually means that the collisions of the test chain with the surrounding chains are not simply added to produce a white-noise force, even when the excluded-volume interactions are screened out [4]. Indeed, we will show that the interactions introduce a new dynamic regime for the range  $2D/(2 - D) < d < 4D/(2 - D)$ . This new regime is derived on different grounds to those proposed by Schweizer [5, 6]. We describe the polymeric manifolds below only in terms of connectivity and excluded volumes. The connectivity defines the  $D$ -dimensional subspace which is embedded in the Euclidean space with  $d$  dimensions. The chains or manifolds in our consideration are crossable, so entanglements cannot occur and a reptation dynamics is not considered.

The second general problem, related to the dynamics of the collective variables, can be formulated as the following question: what do the equations of motion for the time-dependent

density correlation and response functions look like? We will derive them by taking into account the density fluctuations around the dynamic random-phase approximation (RPA). The RPA is known to describe several collective phenomena exhibited by interacting polymer systems quite well [7]. At the same time, the theoretical description of the glass transition [8], for instance, is certainly beyond the scope of the RPA, because the interactions become strong and dominant on short length scales. Hence the main aim is to develop a method which allows one to study the glass transition of an ensemble of ‘Rouse chains’ with a degree of polymerization below the critical molecular weight  $N_e$ .

The paper is organized as follows. Section 2 is devoted to one-chain dynamics in the melt, considered on the basis of the generalized Rouse equation. In section 3 the multi-chain or collective dynamics is discussed in relation to the glass transition mode-coupling approach [8]. Finally, in section 4 we discuss the main results.

## 2. The one-chain (manifold) dynamics in the melt

Let us start with a melt of  $D$ -dimensional manifolds in a  $d$ -dimensional space. The test manifold is represented by the  $d$ -dimensional vector  $\mathbf{R}(\vec{x}, t)$  together with the  $D$ -dimensional vector  $\vec{x}$  of the internal coordinates. In the same way, the manifolds of the surrounding matrix are specified by  $\mathbf{r}^{(p)}(\vec{x}, t)$  ( $p = 1, 2, \dots, M$ ). We have chosen the notation in such a way that the bold italic characters describe the external degrees of freedom in Euclidean  $d$ -dimensional space, whereas the vectors indicated by arrows correspond to the internal  $D$ -dimensional space. The model of the melt of  $M$  (monodisperse) tethered manifolds used in the following is based on the generalized Edwards Hamiltonian:

$$H = \frac{1}{2}\varepsilon \sum_{p=1}^M \int d^D x (\nabla_{\vec{x}} \mathbf{r}^{(p)}(\vec{x}))^2 + \frac{1}{2} \sum_{p,p'=1}^M \int d^D x \int d^D x' V[\mathbf{r}^{(p)}(\vec{x}) - \mathbf{r}^{(p')}(\vec{x}')] \quad (1)$$

where  $\varepsilon = dT/l^2$  is the elastic modulus for the Kuhn segment length  $l$ . The model that we have chosen allows interpolation between linear polymer chains, which correspond to  $D = 1$ , tethered membranes ( $D = 2$ ), and three-dimensional polymer networks ( $D = 3$ ) (see figure 1). Following analytic continuation to rational-number values of  $D$ , statements regarding polymeric fractals can be made. Branched polymers (and percolation clusters) correspond closely to the dimension  $D = 4/3$  [9]. In the melt of  $M$  species, an additional (test) manifold is immersed, which is described by the variables  $\mathbf{R}(\vec{x}, t)$ . The total number of beads is given by  $\mathcal{N} = N \times N \times \dots \times N$  ( $D$  factors).

The corresponding Langevin equations in Cartesian components  $j$  for the test chain have the forms

$$\xi_0 \frac{\partial}{\partial t} R_j(\vec{x}, t) - \varepsilon \Delta_x R_j(\vec{x}, t) + \frac{\delta}{\delta R_j(\vec{x}, t)} \int d^D x' V(\mathbf{R}(\vec{x}, t) - \mathbf{R}(\vec{x}', t)) + \frac{\delta}{\delta R_j(\vec{x}, t)} \sum_{p=1}^M \int d^D x' V(\mathbf{R}(\vec{x}, t) - \mathbf{r}^{(p)}(\vec{x}', t)) = f_j(\vec{x}, t) \quad (2)$$

and

$$\xi_0 \frac{\partial}{\partial t} r_j^{(p)}(\vec{x}, t) - \varepsilon \Delta_x r_j^{(p)}(\vec{x}, t) + \frac{\delta}{\delta r_j^{(p)}(\vec{x}, t)} \sum_{m=1}^M \int d^D x' V(\mathbf{r}^{(p)}(\vec{x}, t) - \mathbf{r}^{(m)}(\vec{x}', t)) + \frac{\delta}{\delta r_j^{(p)}(\vec{x}, t)} \int d^D x' V(\mathbf{r}^{(p)}(\vec{x}, t) - \mathbf{R}(\vec{x}', t)) = \tilde{f}_j(s, t) \quad (3)$$

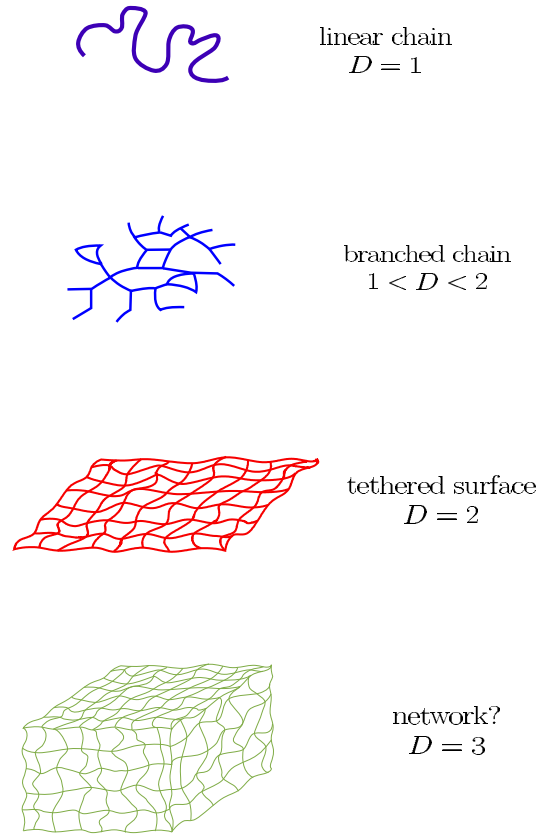


**Figure 1.** The manifold model includes the cases intermediate between the linear polymer chain and the polymer network. It should be stressed that the case of  $D = 3$  is ill defined for the Gaussian model, since the fractal dimension goes negative. This is in accordance with the fact that three-dimensional networks collapse if no excluded volume is present.

where  $\xi_0$  is the bare friction coefficient,  $V(\cdot \cdot \cdot)$  is the excluded-volume interaction function,  $\Delta_{\vec{x}}$  denotes a  $D$ -dimensional Laplacian in internal space, and the random forces have the standard Gaussian distribution.

We find it more convenient to reformulate the Langevin problem (2), (3) in the Martin–Siggia–Rose (MSR) functional integral representation [10]. This representation is especially useful for performing transformations to collective variables or integration over a subset of variables. In our case, we introduce the matrix density  $\rho(\mathbf{r}, t)$  and the response-field density  $\pi(\mathbf{r}, t)$ :

$$\rho(\mathbf{r}, t) = \sum_{p=1}^M \int d^D x \delta(\mathbf{r} - \mathbf{r}^{(p)}(\vec{x}, t)) \quad (4)$$

$$\pi(\mathbf{r}, t) = \sum_{p=1}^M \sum_{j=1}^d \int d^D x i \hat{r}_j^{(p)}(\vec{x}, t) \nabla_j \delta(\mathbf{r} - \mathbf{r}^{(p)}(\vec{x}, t)). \quad (5)$$

In reference [11], the first systematic expansion of the effective action in the MSR functional integral in terms of  $\rho$  and  $\pi$  was given.

The aim now is to integrate out the matrix variables (4), (5). To do this, we carry out

the expansion of the effective action up to second order with respect to  $\rho$  and  $\pi$ , which corresponds to the random-phase approximation (RPA). After performing the (Gaussian) functional integration, all information about the matrix is subsumed in the RPA correlation ( $S_{00}(\mathbf{k}, t)$ ) and response ( $S_{01}(\mathbf{k}, t)$ ) functions [12].

The resulting action still includes the test-manifold variables in a highly non-linear way. In order to handle this, we use a Hartree-type approximation and also take into account the fluctuation-dissipation theorem for both the test manifold and the matrix variables. This strategy leads (see [12] for details) to the following generalized Rouse equation (GRE):

$$\xi_0 \frac{\partial}{\partial t} R_j(\vec{x}, t) + \int d^D x' \int_0^t dt' \Gamma(\vec{x}, \vec{x}'; t - t') \frac{\partial}{\partial t'} R_j(\vec{x}', t') - \int d^D x' \Omega(\vec{x}, \vec{x}') R_j(\vec{x}', t) = \mathcal{F}(\vec{x}, t) \quad (6)$$

with the memory function

$$\Gamma(\vec{x}, \vec{x}'; t) = \frac{1}{T} \int \frac{d^d k}{(2\pi)^d} k^2 |V(\mathbf{k})|^2 F(\mathbf{k}; \vec{x}, \vec{x}'; t) S_{00}(\mathbf{k}, t) \quad (7)$$

and the effective static elastic susceptibility

$$\Omega(\vec{x}, \vec{x}') = \varepsilon \Delta(\vec{x} - \vec{x}') \delta_x - \int \frac{d^d k}{(2\pi)^d} k^2 \mathcal{V}(\mathbf{k}) \left[ F_{st}(\mathbf{k}; \vec{x}' \vec{x}') - \delta(\vec{x} - \vec{x}') \int d^D x'' F_{st}(\mathbf{k}; \vec{x}, \vec{x}'') \right] \quad (8)$$

and the random force  $\mathcal{F}(\vec{x}, t)$  has the correlator

$$\langle \mathcal{F}(\vec{x}, t) \mathcal{F}(\vec{x}', t') \rangle = 2T \delta_{ij} [\xi_0 \delta(\vec{x} - \vec{x}') \delta(t - t') + \Theta(t - t') \Gamma(\vec{x}, \vec{x}'; t - t')]. \quad (9)$$

In equation (8), the effective interaction function

$$\mathcal{V}(\mathbf{k}) = V(\mathbf{k}) \left[ 1 - \frac{1}{T} V(\mathbf{k}) S_{st}(\mathbf{k}) \right] \quad (10)$$

takes the standard screened form [4]

$$\mathcal{V}(\mathbf{k}) = \frac{V(\mathbf{k})}{1 + V(\mathbf{k}) F_{st}^{(0)}(\mathbf{k})/T} \quad (11)$$

(where  $F_{st}^{(0)}(\mathbf{k})$  is the free-system correlator), if the standard RPA result is used for the melt static correlator  $S_{st}(\mathbf{k})$ .

It is an important point that we treat the static and dynamic parts of the GRE (6) on an equal footing. The static behaviour is determined mainly by the effective static susceptibility (8). That is, when the second term on the r.h.s. of equation (8) (which comes from the interaction with the melt) is not relevant, then the manifold is Gaussian. This holds for

$$d > d_{uc} = \frac{2D}{2 - D} \quad (12)$$

where  $d_{uc}$  is the static upper critical dimension. The corresponding Gaussian fractal dimension has the same form:  $d_f^0 = 2D/(2 - D)$ . Also, the necessary condition  $d_f^0 < d$  immediately implies that  $D < D_s = 2d/(2 + d)$ . The *upper critical dimension*  $d_{uc}$  in a melt and the *spectral critical dimension*  $D_s$  were discussed first in [13]. For  $d < d_{uc}$ , the second term on the r.h.s. of equation (8) is dominant, and the system becomes unstable. The manifold is saturated in a melt, i.e. it loses its fractal nature and becomes compact [13]. Let us consider the dynamics at  $d \geq d_{uc}$ . We restrict the discussion to mainly the mean square displacement of the centre of mass:

$$O_{cm}(t) = \langle [R_{cm}(t) - R_{cm}(0)]^2 \rangle \propto t^w \quad (13)$$

where  $w$  is a corresponding exponent.

The renormalized Rouseian regime occurs when the memory kernel in equation (6) dominates the Stokes friction term. In the RPA, the melt density correlator  $S_{00}(\mathbf{k}, t)$  is well approximated by

$$S_{00}(\mathbf{k}, t) = S_{\text{st}}(\mathbf{k}) \times \begin{cases} \exp\{-k^2 D_{\text{coop}}(\mathbf{k})t\} & (kl)^{d_f} \mathcal{N} \ll 1 \\ \exp\left\{-\frac{k^2 l^2}{2d} \left(\frac{t}{\tau_0}\right)^{2z_0}\right\} & (kl)^{d_f} \mathcal{N} \gg 1 \end{cases} \quad (14)$$

where the cooperative diffusion coefficient  $D_{\text{coop}}(\mathbf{k}) = \rho V(\mathbf{k})/\xi_0$ ,  $z_0 = (2 - D)/4$ , and  $\tau_0 = \xi_0 l^2 / Td$ .

If we assume that for a relatively small displacement,  $l^2 < Q_{\text{cm}} < R_G^2$ , the main contribution to the integral (7) comes from the large wave vectors,  $(kl)^{d_f} \mathcal{N} \gg 1$ , then we obtain

$$Q_{\text{cm}}(t) = \frac{D_0}{\mathcal{N}} \left(\frac{t}{\tau_0}\right)^w \quad (15)$$

where  $D_0 = l^2 \epsilon A / \Gamma(w + 1)$  ( $\Gamma(x)$  is the gamma function) and

$$w = \beta = z_0(d - d_{\text{uc}} + 2). \quad (16)$$

The condition of the memory term dominance immediately defines the *dynamic upper critical dimension*:

$$\tilde{d}_{\text{uc}} = \frac{4D}{2 - D} = 2d_{\text{uc}} \quad (17)$$

i.e. the dimension above which the manifold exhibits the simple Rouse behaviour; at  $d = \tilde{d}_{\text{uc}}$  one can call it marginal Rouse behaviour, and only for  $d < \tilde{d}_{\text{uc}}$  is the dynamic exponent  $w$  renormalized.

In the large-displacement regime,  $R_G^2 \ll Q_{\text{cm}}$ , one can assume that only small wave vectors,  $(kl)^{d_f} \mathcal{N} \ll 1$ , are relevant. In this case the dynamics of the matrix (melt) is driven mainly by the cooperative diffusion coefficient  $D_{\text{coop}}$ . For the memory kernel, the calculation yields

$$\int d^D x d^D x' \int_0^\infty dt \Gamma(x, x'; t) \propto [D_{\text{coop}}]^{-1} \mathcal{N}^{(1-d/d_f)}. \quad (18)$$

But  $D_{\text{coop}} = \mathcal{O}(N^0)$  and  $d_f^0 < d$ ; thus the memory term becomes irrelevant and the simple Rouse result does not change.

In figure 2 we have summarized the overall schematic behaviour for  $Q_{\text{cm}}(t)$ . At relatively short times,  $\tau_0 < t \ll \tau_R$ , and for relatively small displacements,  $l^2 < Q_{\text{cm}}(t) \ll R_G^2$ , the test-chain dynamics is mainly determined by the fluctuations from the interval  $(kl)^{d_f} \mathcal{N} \gg 1$ . As a result, the renormalized Rouseian behaviour dominates, and, e.g. for the melt of polymer chains ( $D = 1$ ) in three-dimensional space, the exponent  $w = 3/4 = 0.75$ . In the opposite limit, i.e. when  $\tau_R \ll t$  and  $R_G^2 \ll Q_{\text{cm}}(t)$ , the long-wavelength fluctuations  $(kl)^{d_f} \mathcal{N} \ll 1$  are relevant and the melt has almost no influence on the test chain: the simple Rouse regime is recovered. MC simulations of the bond-fluctuation model [14] as well as MD simulations [15] of the athermal melt have been undertaken. Recently, the static and dynamic properties of a realistic polyethylene melt have also been studied [2, 3]. In both MC and MD simulations, a subdiffusional regime for the centre of mass at intermediate times is clearly observable. It was found e.g. that, for the chain length  $N = 200$  and for relatively short times,  $Q_{\text{cm}}(t) \propto t^w$  with  $w = 0.8$  (instead of  $w = 1$  for the Rouse regime) according to [14] or  $w = 0.71$  according to [15]. This deviation from the simple Rouse regime also occurs for short chains ( $N < N_c$ ), which clearly are not entangled [2, 3].

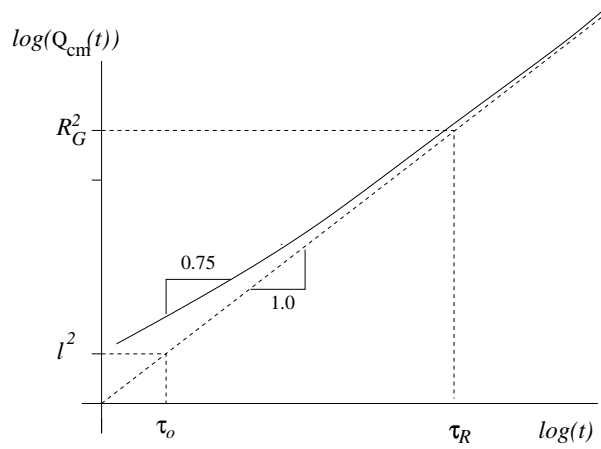


**Figure 2.** A schematic plot of  $Q_{\text{cm}}(t)$  for the simple Rouse (dashed line) and the renormalized Rouse (solid curve) dynamics.

### 3. The collective dynamics

Now we are interested in the equations of motion (which would go the beyond RPA) for the full correlation:

$$G_{00}(\mathbf{k}; t, t') = \langle \rho(\mathbf{k}, t) \rho(\mathbf{k}, t') \rangle \quad (19)$$

and the two response functions:

$$G_{01}(\mathbf{k}; t, t') = \langle \rho(\mathbf{k}, t) \pi(\mathbf{k}, t') \rangle \quad \text{for } t > t' \quad (20)$$

$$G_{10}(\mathbf{k}; t, t') = \langle \pi(\mathbf{k}, t) \rho(\mathbf{k}, t') \rangle \quad \text{for } t < t' \quad (21)$$

where the collective variables  $\rho$  and  $\pi$  are given by equations (4) and (5). The starting point is the Langevin equation (3) for the melt manifolds. By making use of the standard MSR functional integral representation, after transformation to the collective variables (4) and (5) we arrive at the generating functional (GF) which looks like a functional integral over these variables [11]. This is a very compact field theoretical formulation of the full Langevin dynamics. The exact form of the ‘effective action’ in this GF is not known explicitly, but can be obtained by a functional expansion. This expansion can be done under the assumption that the density fluctuations are not very large and the ‘effective action’ is convex [11]. As a result, the GF takes into account fluctuations around the RPA up to arbitrary order (see equation (27) in reference [11]). This GF is the dynamic generalization of the coarse-grained partition function which was obtained (for a block copolymer melt) in reference [16].

From this GF, the equations of motion for the correlation and response functions (19)–(21) can be derived in the standard way [17]. As a result, we have

$$\left[ \tau_c \frac{\partial}{\partial t} + \chi_{\text{st}}^{-1}(\mathbf{k}) \right] G_{01}(\mathbf{k}; t, t') + \int_{t'}^t \Sigma_{10}(\mathbf{k}; t, t'') G_{01}(\mathbf{k}; t'', t') dt'' = -\delta(t - t') \quad (22)$$

$$\begin{aligned} \left[ \tau_c \frac{\partial}{\partial t} + \chi_{\text{st}}^{-1}(\mathbf{k}) \right] G_{00}(\mathbf{k}; t, t') + \int_{-\infty}^t \Sigma_{10}(\mathbf{k}; t, t'') G_{00}(\mathbf{k}; t'', t') dt'' \\ + \int_{-\infty}^t \Sigma_{11}(\mathbf{k}; t, t'') G_{10}(\mathbf{k}; t'', t') dt'' = -2T\tau_c G_{10}(t, t'). \end{aligned} \quad (23)$$

In equations (22) and (23), the inverse RPA static susceptibility

$$\chi_{\text{st}}^{-1}(\mathbf{k}) = [\beta F_{\text{st}}(\mathbf{k})]^{-1} - V(k) \quad (24)$$

and  $\tau_c$  is the bare correlation time. The matrix elements  $\Sigma_{10}$  and  $\Sigma_{11}$  are so-called ‘self-energy’ functionals and their representations contain only one-line irreducible diagrams (or diagrams which cannot be disconnected by cutting only one line) [17]. Equations (22) and (23) are very general. Qualitatively, the same equations of motion were obtained for a test chain in a melt [10], for a manifold in a random medium [18], and for some spin systems [19]. Now let us assume that the fluctuation-dissipation theorem (FDT) is valid for the correlator and response function:

$$\frac{1}{T} \frac{\partial}{\partial t} G_{00}(\mathbf{k}, t) = G_{01}(\mathbf{k}, t) - G_{10}(\mathbf{k}, t) \quad (25)$$

as well as for the ‘self-energy’

$$\frac{1}{T} \frac{\partial}{\partial t} \Sigma_{11}(\mathbf{k}, t) = \Sigma_{10}(\mathbf{k}, t) - \Sigma_{01}(\mathbf{k}, t). \quad (26)$$

Then equations (22) and (23) are reduced to the Mori–Zwanzig equation for the correlation function derived by the projection formalism [20]. After performing the Laplace transformation with respect of time, this equation for  $\phi(\mathbf{k}, z) \equiv G_{00}(\mathbf{k}, z)/G_{\text{st}}(\mathbf{k})$  takes the form

$$\phi(\mathbf{k}, z) = \left( -iz + \frac{k^2 G_{\text{st}}^{-1}(\mathbf{k})}{\tau_0 + k^2 M(\mathbf{k}, z)} \right)^{-1} \quad (27)$$

where  $\tau_0 = \xi_0/T\rho_0$  and the memory kernel

$$M(\mathbf{k}, z) = \frac{1}{T^2} \Sigma_{11}(\mathbf{k}, z). \quad (28)$$

Equations (27) and (28) have been used for the ideal-glass-transition problem [8]. In this case the correlator  $G_{00}(\mathbf{k}, z)$  and the memory kernel  $M(\mathbf{k}, z)$  each acquire a pole at  $z = 0$  at a critical temperature  $T_c$ . One can easily see that such contributions come from the sum of all ‘water-melon’ diagrams, which are represented in figure 3. Each line denotes the full matrix  $G_{\alpha\beta}(\mathbf{k}, z)$ , and a vertex with  $m$  legs denotes the bare vertex function  $W_{\alpha\beta\dots\gamma}^{(m)}(\mathbf{k}_1, z_1; \mathbf{k}_2, z_2; \dots; \mathbf{k}_m, z_m)$ , the expressions for which are given in [11]. The mode-coupling approximation (MCA) corresponds to the case where for all of the vertices renormalization is neglected [19].

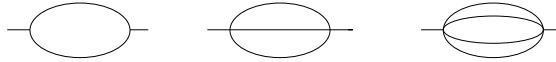


**Figure 3.** A diagrammatic representation of the self-energy  $\Sigma_{11}(\mathbf{k}, z)$  in the MCA, which has a simple pole at  $z = 0$ , i.e. is relevant for the ideal-glass transition. The vertices  $W^{(3)}, W^{(4)}, \dots$  are bare; i.e. this approximation neglects all vertex renormalization.

The explicit expression for the arbitrary vertex function  $W_{\alpha\beta\dots\gamma}^{(n)}(1, 2, \dots, n)$  is not known in detail, and one cannot sum all ‘water-melon’ diagrams. That is why in the spirit of the MCA we restrict our consideration to the first diagram given in figure 3, which corresponds to the one-loop approximation. As a result, we have

$$M(\mathbf{k}, z) = 2 \left( \frac{1}{4!} \right)^2 \frac{1}{\rho_0^4 N^2} \int \frac{d^3 q \, ds}{(2\pi)^4} \left[ 3 + \frac{Nl^2}{6} (k^2 + q^2 + \mathbf{k} \cdot \mathbf{q}) \right]^2 G_{\text{st}}(-\mathbf{k} - \mathbf{q}) G_{\text{st}}(\mathbf{q}) \times \phi(-\mathbf{k} - \mathbf{q}, -z - s) \phi(\mathbf{q}, s). \quad (29)$$



Equation (27) with the memory kernel (29) qualitatively corresponds to the result from the conventional mode-coupling theory (MCT), although the kernel of the integral part has a different form (see e.g. equation (3.37) in reference [8]). In reference [8], on the basis of bifurcation theory, the solution of integral equations of this type has been analysed in full detail. It was, in particular, shown that a positive solution for the so-called non-ergodicity parameter exists provided that the memory kernel of the integral part is positive, and symmetric in  $k$  and  $q$  (see sections 3.6 and 3.7 in [8]). One can see that equation (29) fits these conditions. It has also been shown in [8] that close to the bifurcation point all correlations show the universal scaling behaviour. We are not in a position to discuss here the different scenarios of the idealized-glass transition and instead refer readers to reference [8].

#### 4. Discussion

We have shown that for  $d > d_{uc}$  the excluded-volume interaction is screened out and the manifold is Gaussian with the fractal dimensionality  $d_f^0 = 2D/(2 - D)$ . Nevertheless, the dynamic behaviour is renormalized whenever  $d_{uc} < d < \tilde{d}_{uc}$ , where  $\tilde{d}_{uc}$ , the *dynamic upper critical dimension*, is given by equation (17), i.e. the reactive and the dissipative forces in GRE are not screened out simultaneously. For example, for the melt of polymer chains ( $D = 1$ )  $d_{uc} = 2$  and  $\tilde{d}_{uc} = 4$ , and in the three-dimensional space one should expect the Gaussian static behaviour but the renormalized Rousean dynamics. Why do two upper critical dimensions exist? This can be simply seen from the estimate of the energy which corresponds to the effective contacts. For the static case, the scaling of this energy yields [13]

$$U_{\text{stat}} \propto v_{\text{eff}} \frac{\mathcal{N}^2}{R^d} \propto \frac{v}{\mathcal{N}} \frac{\mathcal{N}^2}{\mathcal{N}^{d/d_f^0}} \propto \mathcal{N}^{1-d/d_f^0} \quad (30)$$

where  $v_{\text{eff}}$  is the screened effective potential and  $v$  is the bare excluded-volume interaction. As one can see, for  $d > d_f^0 = d_{uc}$ ,  $U_{\text{stat}} \rightarrow 0$  and the manifolds are Gaussian.

In contrast, the effective dynamic contacts are effectively ‘short ranged’, and as a result

$$U_{\text{dyn}} \propto v \frac{\mathcal{N}^2}{R^2} \propto \mathcal{N}^{2-d/d_f^0}. \quad (31)$$

This scaling immediately leads to the conclusion that for  $d > \tilde{d}_{uc} = 2d_f^0$  the manifold dynamics is Rousean.

In section 2 we have already discussed some MC and MD simulation results for three-dimensional polymer chain melts ( $d_{uc} = 2$ ,  $\tilde{d}_{uc} = 4$ ). The best test of the renormalized Rouse-dynamics predictions would be a simulation of rather long crossable (to avoid reptation) chains, but still with an excluded-volume interaction. In a recent MC simulation [21], the statics and dynamics of such melts have been studied. Unfortunately, in [21] the plot of  $Q_{\text{cm}}(t)$  is not given explicitly, i.e. it remains unclear from this simulation how the mode  $p \rightarrow 0$  is renormalized.

We have also shown how the general equation of motion for the collective (multi-chain) correlation and response functions can be derived. For the case where the FDT holds, we have arrived at the same type of equation as has been extensively studied in the framework of MCT [8]. For the general off-equilibrium case, the correlation and response functions depend not on the time differences but on both time moments (see equations (22) and (23)). This leads to the so-called *aging phenomena* which have already been investigated theoretically for some simple spin systems [19]. The general equations (22) and (23) are specified for the polymer melt, and could be solved numerically in the MCA.

## References

- [1] Richter D, Willner L, Zirkel A, Fargo B, Fetters L J and Huang J S 1994 *Macromolecules* **27** 7437  
Pearson D S, Fetters L J, Graessly W W, Ver Strate G and von Meerwal E 1994 *Macromolecules* **27** 711
- [2] Paul W, Smith G D and Yoon D Y 1997 *Macromolecules* **30** 7772
- [3] Paul W, Smith G D, Yoon D Y, Fargo B, Rathgeber S, Zirkel A, Willner L and Richter D 1998 *Phys. Rev. Lett.* **80** 2346
- [4] Doi M and Edwards S F 1986 *The Theory of Polymer Dynamics* (Oxford: Clarendon)
- [5] Schweizer K S 1989 *J. Chem. Phys.* **91** 5802  
Schweizer K S 1989 *J. Chem. Phys.* **91** 5822
- [6] Fuchs M and Schweizer K S 1997 *J. Chem. Phys.* **106** 347
- [7] Akcasu A Z, Benmouna M and Benoit H 1986 *Polymer* **27** 1953  
Borsali R, Fischer E W and Benmouna M 1991 *Phys. Rev. A* **43** 5732
- [8] Götze W 1991 *Liquids, Freezing and Glass Transition* ed J-P Hansen, D Levesque and J Zinn-Justin (Amsterdam: North-Holland)
- [9] Alexander S and Orbach R 1982 *J. Physique Lett.* **43** L625
- [10] Rehkopf M, Rostiashvili V G and Vilgis T A 1997 *J. Physique II* **7** 1469
- [11] Rostiashvili V G, Rehkopf M and Vilgis T A 1998 *Eur. Phys. J. B* **6** 233  
(Rostiashvili V G, Rehkopf M and Vilgis T A 1997 *Preprint cond-mat/9710156*)
- [12] Rostiashvili V G, Rehkopf M and Vilgis T A 1999 *J. Chem. Phys. B* **110** 639  
(Rostiashvili V G, Rehkopf M and Vilgis T A 1998 *Preprint cond-mat/9809350*)
- [13] Vilgis T A 1987 *Phys. Rev. A* **36** 1506  
Vilgis T A 1988 *Physica A* **153** 341  
Vilgis T A 1992 *J. Physique II* **2** 1961  
Haronka P and Vilgis T A 1995 *J. Chem. Phys.* **102** 6586
- [14] Paul W, Binder K, Heermann D W and Kremer K 1991 *J. Chem. Phys.* **95** 7726
- [15] Smith S W, Hall C K and Freeman B D 1996 *J. Chem. Phys.* **104** 5616
- [16] Ohta T and Kawasaki K 1986 *Macromolecules* **19** 2621  
Fredrickson G H and Helfand E J 1987 *J. Chem. Phys.* **87** 697
- [17] Zinn-Justin J 1989 *Quantum Field Theory and Critical Phenomena* (Oxford: Clarendon)
- [18] Kinzelbach H and Horner H 1993 *J. Physique I* **3** 1329
- [19] Bouchard J-P, Cugliandolo L, Kurchan J and Mezard M 1996 *Physica A* **226** 243
- [20] Forster D 1992 *Hydrodynamic Fluctuations, Broken Symmetry and Correlation Functions* (Reading, MA: Benjamin)
- [21] Shaffer J S 1994 *J. Chem. Phys.* **101** 4205  
Shaffer J S 1995 *J. Chem. Phys.* **103** 761